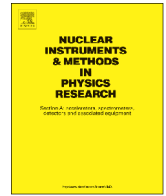




ELSEVIER

Contents lists available at ScienceDirect

Nuclear Instruments and Methods in Physics Research A

journal homepage: www.elsevier.com/locate/nima

Numerical investigations into a fiber laser based dielectric reverse dual-grating accelerator



A. Aimidula^{a,b,*}, C.P. Welsch^{a,b}, G. Xia^{a,c}, K. Koyama^d, M. Uesaka^d, M. Yoshida^e,
O. Mete^{a,c}, Y. Matsumura^d

^a Cockcroft Institute, Daresbury Sci-Tech, Warrington WA4 4AD, United Kingdom

^b Physics Department, University of Liverpool, Liverpool, United Kingdom

^c School of Physics and Astronomy, University of Manchester, Manchester, United Kingdom

^d Department of Nuclear Engineering and Management, The University of Tokyo, Tokai 319-1188, Japan

^e High Energy Accelerator Research Organization (KEK), Tsukuba, Ibaraki 305-0801, Japan

ARTICLE INFO

Available online 11 November 2013

Keywords:

Dielectric accelerator

Dual-grating

Fibre laser

ABSTRACT

Dielectric laser accelerators (DLAs) have great potential for applications, since they can generate acceleration gradients in the range of GeV/m and produce attosecond electron bunches. We described a novel reverse dual-grating dielectric accelerator structure made up of Silicon which is expected to improve beam confinement, and make fabrication easier. Numerical simulation results show that this structure effectively manipulates the laser field and generates a standing wave in the vacuum channel with a phase velocity synchronized to relativistic particles travelling through the structure. Optimum pillar height and channel width have been determined. All required laser parameters and initial particle energy have been analytically estimated and a suitable laser as an energy source is proposed. Finally, the effect of fabrication error on the acceleration gradient is discussed.

© 2013 Elsevier B.V. All rights reserved.

1. Introduction

Since the transverse dimensions of the acceleration cavity of DLAs are on the operating laser wavelength scale, they are able to deliver nm-beams of sub-fs pulses. These high quality beams have a unique advantage for investigating the basic radiobiology processes as they are able to target a single DNA strand [1]. Due to higher damage threshold of dielectric materials, DLAs can produce higher acceleration gradients than conventional microwave accelerators [2–7]. Development of ultrafast laser technology and precise control of the optical phase within the laser pulse is important for future DLA development [8]. There are currently three main candidates for DLA structures: the dual-grating structure [9,10], photonic crystal fibers [11] and the woodpile structure [12]. Significant progress has been made in the fabrication of prototypes of these accelerator structures with nanometer-level precision at low cost with existing nanotechnology such as photolithography and alternate membrane stacking technique [13–16]. An experiment to observe high acceleration gradient in the Micro-Accelerator Platform is recently ongoing [17]. The dual-grating type accelerator has a simpler structure geometry than other types of DLAs and does not suffer group velocity limitation

which results in a rapid slippage of the pulse in photonic band gap accelerator structures [11,18]. Dual-grating acceleration structures also allow a much higher overlapping efficiency of the laser field with the electron beam than semi-open accelerator structures [19]. The power coupling efficiency to the particle bunches can in principle be in the tens of percent, with optimal efficiency at bunch charges of 1 to 20 fC [20].

In this paper, we introduce and analyze a new dual-grating structure based on the original design from Plettner et al. [9], but with the position of pillars slightly changed. The basic working principle of reverse dual-grating structures is based on decreasing the phase velocity of the electric field, thereby synchronizing it with relativistic and non-relativistic electrons. We show that this structure can efficiently modify the laser field, and generates a transverse field which can focus the electron beam locally.

2. Structure geometries and field distribution

The proposed structure cross-section geometry and dimensions are shown in Fig. 1. The lattice length is equal to the wavelength of the operating laser, λ_0 . The dielectric length A and vacuum length B are both equal to $\lambda_0/2$. The wall thickness D is also set to $\lambda_0/2$. Vacuum channel width C and pillar height L are determined by simulations. Electrons move in the vacuum channel (along the Z-axis), while laser light is fed perpendicular to the electron

* Corresponding author at: Cockcroft Institute, Daresbury Sci-Tech, Warrington WA4 4AD, United Kingdom. Tel.: +44 1925 86 40 55.

E-mail address: aimidula.aimierding@liverpool.ac.uk (A. Aimidula).

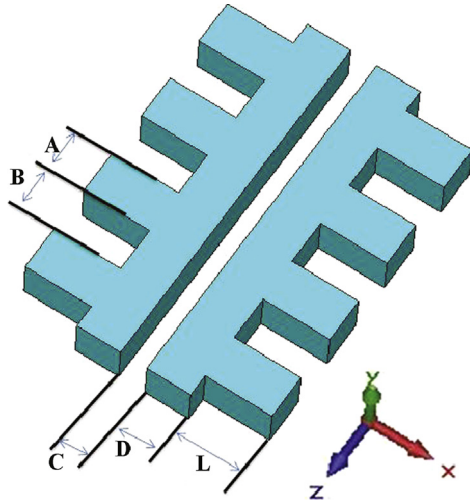


Fig. 1. Dielectric reverse dual-grating structure overview and dimensions, *A* represents dielectric pillar length, *B* represents vacuum length, *C* represents vacuum channel width, *D* represents wall thickness, *L* represents pillar height; $A = B = D = \lambda_0/2$ has been set for all simulations, optimum *C* and *L* are decided by simulations; refractive index $n = 1.527$.

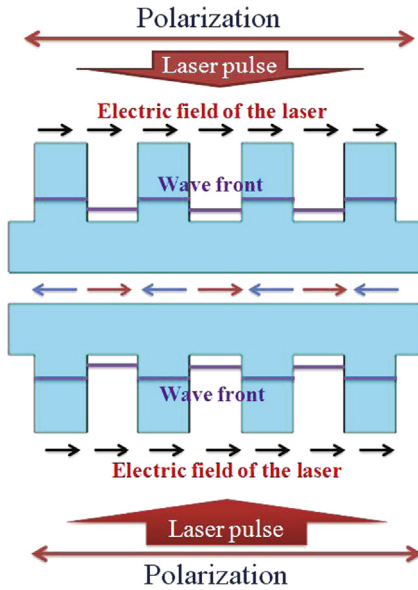


Fig. 2. The working principle of reverse dual-grating accelerator structure.

moving direction from the two facing outer surfaces (along the *X*-axis).

Fig. 2 shows the working principle of reverse dual-grating accelerator structure. As the plane wave of linearly polarized laser light passes through the structure, the light speed in the dielectric grating pillar is lower than that in the adjacent vacuum space. This produces the desired π -phase-delay and a periodic electric field distribution inside the vacuum channel along the longitudinal beam axis.

The wavelength of 1550 nm emitted by an Er-fiber laser was adopted in our simulation because the longer wavelength light ensures larger characteristic length of the structure. The longer wavelength laser is advantageous for the fabrication and the accelerator tuning. We chose a Silica which has a refractive index of $n = 1.527$ [21] at Er laser wavelength. The Silica has good features in transparency, electric field damage threshold, thermal conductivity, nonlinear optical coefficients and chemical stability.

Fig. 3 shows the laser pulse excitation signal shape used for our field calculation. The frequency range is chosen from 1485 nm to

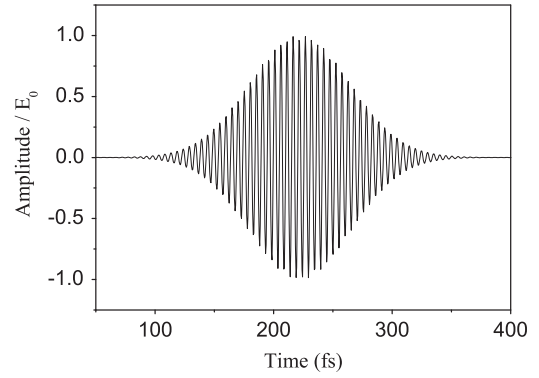


Fig. 3. The temporal shape of electric field of the laser. The full width half maxima (FWHM) of the intensity is 70 fs.

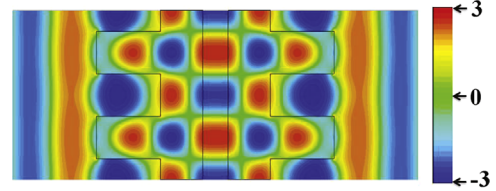


Fig. 4. Electric field *Z*-component peak distribution on the *XZ* plane, colors represent field intensity and directions; $A = B = D = \lambda_0/2$, $C = 0.3\lambda_0$, $L = 0.76\lambda_0$, refractive index of dielectric material $n = 1.527$ has been set for this simulation. (For interpretation of the references to color in this figure legend, the reader is referred to the web version of this article.)

1613 nm. Note that all structure lengths in this paper are normalized by the operating laser wavelength λ_0 , and all field strengths are normalized by the operating laser amplitude E_0 .

Fig. 4 shows the *Z*-component of the electric field peak distribution on the *XZ* plane, where the *Z*-axis corresponds to the longitudinal electron beam direction, and the *X*-axis corresponds to the laser travelling direction. Along the vacuum channel shows the periodic field reversal, and regions of the oscillating electric field of opposite polarity are spaced by $\lambda_0/2$. Consequently relativistic electrons are synchronized with the oscillating field which has a phase velocity equal to the speed of light in vacuum and are accelerated. The optimum pillar height and vacuum channel gap are determined in simulation studies. For the electric field calculation we used CST Microwave Studio [22]. A structure picture has been inserted in **Figs. 5–7**; the dashed line represents the central line of the vacuum channel, the solid line represents the arbitrary axis where we estimate the electric field distribution on it. **Fig. 5** shows the electric field *Z*-component E_Z peak distribution on the central axis along the vacuum channel. From this figure one can see that not only the phase is manipulated by the periodic structure, but also the field amplitude is efficiently adjusted. Due to the diffraction effect, light is focused in the high refractive index region. The E_Z maximum value is found at the center part of the narrow gap surface and is shown in **Fig. 5** as an absolute value of $|E_{max}| \sim 2.5E_0$. The electric field $E_Z \sim 0$ at $1/4\lambda_0$ and $3/4\lambda_0$ points, and this is expected since it guarantees that the relativistic electrons receive an acceleration force all the time.

Fig. 6 shows that this mechanism of feeding the laser from two sides efficiently decreases the transverse field, i.e. the *X*-component of the laser field which is perpendicular to the electron beam travelling direction. The *X*-component is therefore unusable for longitudinal acceleration. The electric field *X*-component E_X on the boundary line between the dielectric pillar and the vacuum space where it appears to be a maximum value is shown in **Fig. 6**. In the two side feeding case, $E_X = 0$ appears at the center of the vacuum channel, and the field has a smaller *X*-component than the one

Download English Version:

<https://daneshyari.com/en/article/8177313>

Download Persian Version:

<https://daneshyari.com/article/8177313>

[Daneshyari.com](https://daneshyari.com)